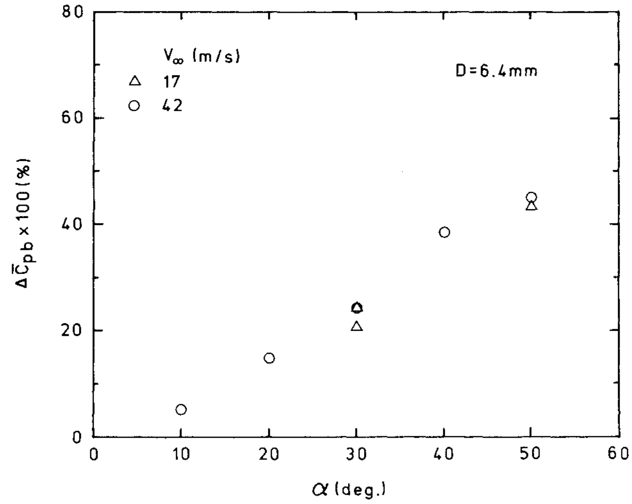

Fig. 4 Variation in average base pressure coefficient vs groove angle ($D = 6.4$ mm).

at 2.5 cm upstream of the base indicated fully developed turbulent boundary layers for $V_\infty = 17$ m/s (δ for upper and lower surfaces of 1.7 and 1.8 cm, respectively). Transverse velocity surveys at the same location indicated the presence of two-dimensional flow over the model between $z/s = 0.25$ and 0.75. Variations in freestream static pressure between the upper and lower surfaces correspond to variations in V_∞ of 1.3% at 17 m/s and 3% at 42 m/s. Model base pressure was measured using 25 pressure taps located along the centerline of the model base. In order to determine the effects of groove angle and groove depth on base pressure, models were tested with groove angles of 10 to 50 deg and groove depths of 3.2 to 9.5 mm (D/δ of 0.2 to 0.6).

Results and Discussion

Base pressure coefficient C_{pb} is presented in Figs. 2 and 3 ($V_\infty = 42$ m/s) as a function of the nondimensional distance in the spanwise direction for variable groove angle tests and variable groove depth tests, respectively. It is evident from these figures that as groove angle or groove depth increases, the base pressure also increases. The data exhibit three-dimensional (end) effects that diminish as α (or D) increases. Asymmetries about the model centerline ($z/s = 0.5$) are also noted. Tests with extended sidewalls have shown these to be largely due to three-dimensional end effects. Maximum increases in base pressure (50 to 60%) were obtained with $\alpha = 50$ deg ($D = 6.4$ mm) and $D = 9.5$ mm ($\alpha = 30$ deg) (see Figs. 2 and 3).

The average base-pressure coefficient $\bar{C}_{pb}$ for each geometry tested was calculated from the C_{pb} data using area weighting. Percent changes in $\bar{C}_{pb}$ from the baseline model for the groove angle tests are presented in Fig. 4 for freestream flow speeds of 17 and 42 m/s. The data indicate an almost linear increase in $\bar{C}_{pb}$ with increasing α. (A similar trend with increasing D was obtained). Overlapping of data from the two different Reynolds number tests suggests the independence of the base pressure increases from Re over the test range. In general, the data presented suggest the presence of a relationship between the groove dimensions and the strength of the interaction between the flow in the grooves and the wake flow.

Conclusions

The results reported herein clearly indicate that the base pressure of a blunt trailing-edge airfoil with surface grooves increases with increasing groove depth and angle. Minimally, attached flow in the grooves appears to be the mechanism by which fluid of higher momentum is redirected to the base flow region to effect an increase in the base pressure. A study of the effect of grooves on the lift and total drag of blunt trailing-edge airfoils is needed to further determine their effectiveness in this important application.

Acknowledgment

The subject research was supported by the National Science Foundation under grant MSM 8519116.

References

[1] Hefner, J. N., and Bushnell, D. M., "An Overview of Concepts for Aircraft Drag Reduction," *Special Course on Concepts for Drag Reduction,* NATO Advisory Group for Aerospace Research and Development, AGARD Rpt. No. 654, 1977.

[2] Nash, J. F., Quincy, V. G., and Callinan, J., "Experiments on Two Dimensional Base Flow at Subsonic and Transonic Speeds," London: Her Majesty's Stationery Office, National Physical Laboratory, Aerodynamics Division, NPL Aero. Rpt. 1070-A.R.C. 25 070, 1963.

[3] Werle, M. J., Paterson, R. W., and Presz, W. M., Jr., "Trailing-edge Separation/Stall Alleviation," *AIAA Journal,* Vol. 25, No. 4, 1986, p. 624.

[4] Gai, S. L., and Sharma, S. D., "Vortex Shedding from a Segmented Blunt Trailing-edge Aerofoil in Subsonic Flow," *Proceedings: 9th Australasian Fluid Mechanics Conference,* Auckland, New Zealand: University of Auckland, Dec. 1986, pp. 371–374.

[5] Wood, C. J., "The Effect of Base Bleed on a Periodic Wake," *Journal of the Royal Aeronautical Society,* Vol. 68, July 1964, pp. 477–482.

[6] Zumwalt, G. W., "Experiments on Three-Dimensional Separating-and-Reattaching Flows," AIAA Paper 81-0259, Jan. 1981.

[7] Lin, J. C., Howard, F. G., and Selby, G. V., "Turbulent Flow Separation Control Through Passive Techniques," AIAA Paper 89-0976, March 1989.

[8] Schlichting, H., *Boundary-Layer Theory,* McGraw-Hill, New York, 7th ed., 1987, p. 539.

Unsteady Transonic Cascade Flow with In-Passage Shock Wave

C.-C. Li*
Chung Shan Institute of Science and Technology, Tauyuan, Taiwan, Republic of China
and
A. F. Messiter† and B. van Leer‡
University of Michigan, Ann Arbor, Michigan

Introduction

In Ref. 1, asymptotic solutions were obtained for unsteady transonic flow in a channel with oscillating walls, for small reduced frequency. It was noted that an oscillating shock wave within the channel causes a time-dependent pressure force having a component in phase with the velocity of the walls,

Received Feb. 7, 1989; revision received July 10, 1989. Copyright © 1989 by the American Institute of Aeronautics and Astronautics. All rights reserved.

*Assistant Research Scientist. Member AIAA.

†Professor, Department of Aerospace Engineering. Associate Fellow AIAA.

‡Professor, Department of Aerospace Engineering. Member AIAA.

which would tend to amplify the motion. Since the flow between adjacent blades of a cascade resembles a channel flow,[2] it would seem possible that this effect might contribute to transonic choke flutter in compressors.

The asymptotic solutions, however, have been derived for particular limiting cases, and have been carried out only as far as a first approximation for the time-dependent shock-wave position. The results may be qualitatively useful over a wide parameter range, but probably provide good numerical accuracy for only a relatively narrow range. Thus, of course, it is necessary to have an accurate numerical method for calculation of these flows. If the amplitude of the shock-wave oscillation were small, the unsteady motion could be described by linearized equations representing small unsteady perturbations about the solution to a nonlinear steady-flow problem; calculations of this kind based on the potential equation are described by Verdon.[3] In the present work, the unsteady perturbations are allowed to be as large as the steady-flow disturbances, and the shock-wave displacement may be large. A scheme for solving the unsteady Euler equations has been developed, based in part on some advanced numerical techniques recently introduced in computational aerodynamics; a good review of more standard methods for unsteady cascade flow is given by Acton and Newton.[4] Details of the present method are shown in Ref. 5; certain aspects are also mentioned in a survey of asymptotic theory for internal transonic flows given in Ref. 6. Some numerical results are shown here for a particular case; the relevance of the asymptotic solutions is discussed first.

Asymptotic Solutions

A nondimensional characteristic time is $\tau = (\omega L/a^*)^{-1}$, where ω is an angular frequency, a^* is a critical sound speed, and L is a reference value of the channel width or distance between successive blades in a cascade; then τ^{-1} is a reduced frequency. For simple harmonic pitching oscillations about $x=0$, the blade surfaces are defined by

$$y = \pm\{1 - \epsilon^2 f(x) + \alpha e^{2\pi i t} x/x_1\}$$

for $-x_1 < x < x_1$, where $\epsilon << 1$ and $\alpha << 1$; ϵ^2 is proportional to the blade thickness ratio; α is the amplitude of the blade oscillations; and the time has been made nondimensional with $2\pi/\omega$. For simplicity the blades are taken to have symmetric profile sections, and adjacent blades are oscillating with 180-deg phase difference.

As in Ref. 1, a limiting case is considered where the undisturbed Mach number M_∞ ahead of the cascade differs from 1 by $\mathcal{O}\{\epsilon\}$. In the limit, velocity and pressure changes for $|x| < x_1$, $|y| < 1$ in an unstaggered cascade are nearly the same as in a channel, except within a distance $\mathcal{O}\{\epsilon^{1/2}\}$ of the entrance and exit. The steady-state flow changes are described in a first approximation by one-dimensional flow equations, so an area change $\mathcal{O}\{\epsilon^2\}$ allows acceleration through sonic speed at a "throat." The exit pressure is such that a shock wave is present downstream of this "throat." Special local, or "inner," solutions are needed just downstream of the shock and near the entrance and exit.

For $\tau^{-1} << \epsilon^2$, the flow is quasisteady and in a first approximation the shock wave responds instantaneously to the blade motions. For $\tau^{-1} = \mathcal{O}\{\epsilon^2\}$ and $\epsilon^2 << \tau^{-1} << \epsilon$, the shock-wave motion lags the wall motion but a small disturbance at the exit still reaches the shock wave instantaneously. For $\tau^{-1} = \mathcal{O}\{\epsilon\}$ and $\epsilon << \tau^{-1} << 1$, there is a time lag in the local flow properties as well as in the shock-wave motion. Different choices can be made for the order of magnitude of α; here α is chosen no larger than $\mathcal{O}\{\epsilon^2\}$, and the amplitude of the shock-wave oscillation is found to be $\mathcal{O}\{\tau\alpha/\epsilon\}$. In Ref. 1, solutions were obtained for the special case of parabolic blades when $\tau^{-1} = \mathcal{O}\{\epsilon^2\}$ and $\tau^{-1} = \mathcal{O}\{\epsilon\}$ and the amplitude of the shock-wave motion was $\mathcal{O}(1)$.

If $\alpha = \beta\epsilon^3$, where $\beta = \mathcal{O}(1)$, the first approximation to the resulting shock-wave speed is found from Eqs. (39) and (42) or (65b) of Ref. 1, for $\tau^{-1} = \mathcal{O}\{\epsilon^2\}$ and $\mathcal{O}\{\epsilon\}$, respectively. For the intermediate case $\epsilon^2 << \tau^{-1} << \epsilon$, the appropriate limiting forms of these two results show that the shock wave lags the wall motion by 90 deg. The shock is furthest upstream (or downstream), giving the largest region of subsonic (or supersonic) flow, when the downstream parts of the blades have their maximum outward (or inward) velocity. The pressure changes associated with the shock-wave motion thus give an aerodynamic moment in phase with the blade angular velocity, which has the effect of a negative damping. This contribution can be shown to be $\mathcal{O}\{\alpha/\tau^{-1}\}$, whereas pressure changes away from the shock wave cause changes $\mathcal{O}\{\alpha/\epsilon\}$ in the moment, which are of higher order since $\tau^{-1} << \epsilon$. This effect, however, is predominant only over a limited frequency range. In the quasisteady flow for $\tau^{-1} << \epsilon^2$, the moment is in phase with the blade displacement. For $\tau^{-1} = \mathcal{O}\{\epsilon^2\}$ the moment has components in phase with blade displacement and velocity. For $\tau^{-1} = \mathcal{O}\{\epsilon\}$, contributions of pressure variations away from the shock wave are no longer of higher order. For $\tau^{-1} >> \epsilon$, it does not seem clear which effects are most important.

It is therefore desirable to have a rough idea of the frequencies which might be of practical interest. An equation of motion for small-amplitude torsional oscillations of a blade can be integrated from the blade root to the blade tip to give a two-dimensional linearized aeroelastic model. If the inertia and elastic properties of the blade are assumed uniform, the equivalent torsional spring constant is $K = (\pi/2)GJ$, where GJ is the torsional stiffness; the numerical factor corresponds to a first mode shape in the form of a sine function. The corresponding natural frequency is $(K/I)^{1/2}$, where I is the moment of inertia of the blade profile section about the axis of rotation. Sample numerical values taken from Ref. 7 give a reduced frequency $\tau^{-1} \cong 0.6$. If this is at all representative, the conclusion should probably be that the reduced frequencies of interest are at least $\mathcal{O}\{\epsilon\}$, so that the effect of the shock-wave motion on the moment may or may not be dominant.

Numerical Calculations

A finite-volume scheme has been developed[5] to solve the unsteady Euler equations for cascade geometries. The basis of the scheme is a piecewise-linear spatial distribution of the flow variables,[8] the time evolution of which is computed with a predictor-corrector method.[9] The overall scheme achieves second-order accuracy in regions of smooth flow and is implemented on a moving grid. The numerical fluxes at cell interfaces used in the final update (corrector) step are based on Van Leer's flux-vector splitting,[10] reformulated for a moving grid by Anderson et al.[11] This makes the method an upwind-differencing scheme, leading to greater robustness, lower dispersion errors, and optimum representation of normal shocks. Spurious oscillations near shock waves are prevented by limiting the magnitude of the gradients of the linear distributions used in the cells; the particular limiter is described in Ref. 9. The cascade is simulated by a periodic spatial boundary condition across two channels, while Hedstrom's[12] time-dependent absorbing boundary procedure is used at the downstream computational boundary in order to avoid numerical reflections. More elaborate and more effective nonreflecting boundary procedures, such as discussed by Giles,[13] may be implemented, but this was not judged necessary for the flow cases studied.

Calculations have been carried out primarily for a reduced frequency $\tau^{-1} = 0.1$, a small enough value that the asymptotic results should probably be relevant. Figure 1 shows results for pitch oscillations of a parabolic blade with 5% thickness ratio;

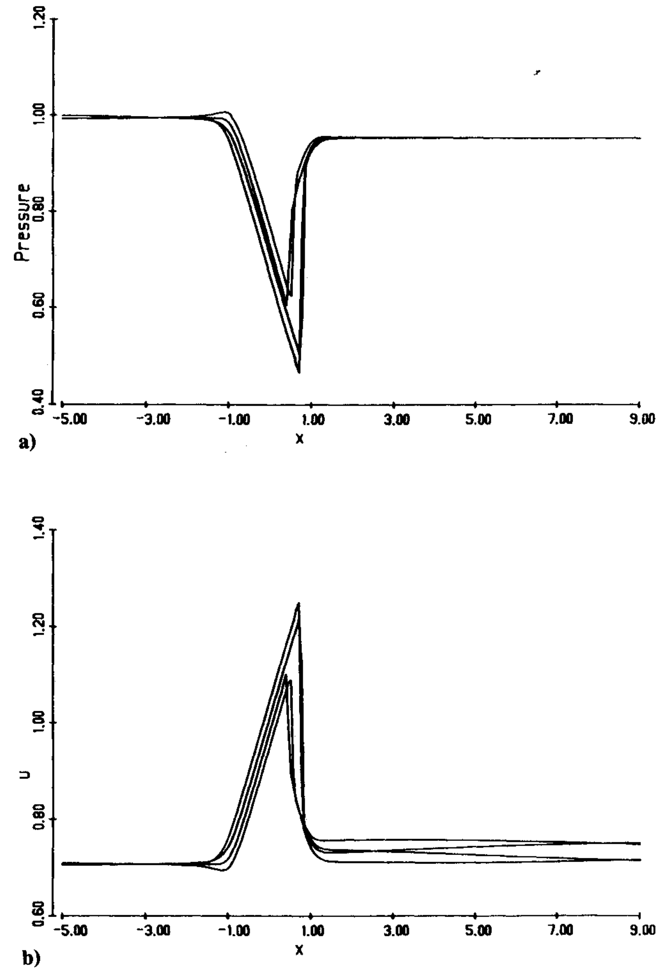

Fig. 1 Unstaggered cascade having parabolic blades of 5% thickness oscillating in pitch with reduced frequency 0.1, amplitude 1 deg, and 180-deg phase difference, at times spaced one-quarter period apart: a) centerline pressure; and b) centerline velocity.

the nondimensional blade half-chord is $x_1 = 1$, so that the chord length equals twice the spacing between blades, and the leading and trailing edges are located at $x = \pm 1$. The centerline pressure and velocity are shown as functions of x at values of time one-quarter period apart, for an oscillation amplitude of 1 deg, at an upstream Mach number $M_\infty = 0.678$, the value required for choking. The shock wave is captured in one or two cells, with no spurious oscillations. Ahead of the shock, the pressure perturbation is very nearly proportional to the velocity perturbation, in agreement with the low-frequency linearized prediction. Downstream of the exit, the pressure is constant, but the velocity shows small variations, indicating that the time derivative in the unsteady Bernoulli equation is not really negligible here. Disturbances are carried downstream rapidly, so that the velocity varies only very slowly with distance.

In order to demonstrate agreement of the asymptotic and numerical solutions when flow perturbations are sufficiently small, the shock-wave position is shown in Fig. 2 as a function of time for pitch oscillations of a parabolic blade with 2% thickness ratio and oscillation amplitude 0.1 deg. In this case, the agreement is seen to be fairly good, with some error in phase; the higher-frequency waviness evident in the figure is a result of the interpolation of the cell-averaged local Mach number. For the larger thickness and amplitude of Fig. 1, however, the asymptotic prediction for the amplitude of the shock-wave motion is found to be about twice the numerical value[5]; a partial derivation of higher-order terms suggests that a full solution for terms of the next order would improve the agreement significantly.

Similar calculations, not shown here but included in Refs. 5 and 6, have been carried out for a higher frequency $\tau^{-1} = 0.5$, thickness ratio 5%, and larger oscillation amplitude 2.5 deg. (In Ref. 6, the captions for Figs. 7–9 state the amplitude incorrectly as 0.25 deg.) The results indicate that the pressure and velocity are no longer proportional ahead of the shock; downstream of the exit the pressure is again nearly constant, but the velocity perturbations are larger and have shorter wavelength.[5,6] For these reasons, the frequency $\tau^{-1} = 0.5$, although perhaps small, should clearly be considered $\mathcal{O}(1)$ rather than $\mathcal{O}\{\epsilon\}$. The shock-wave position is no longer close to a sine curve, as in Fig. 2, and shows a kind of transient behavior that lasts for several cycles before a steady-state periodic motion is observed. This effect can in fact be predicted,[5] at least qualitatively, by a partial higher-order solution for $\tau^{-1} = \mathcal{O}\{\epsilon\}$. The numerical solution for the pressure at $x = x_1$ for $\tau^{-1} = 0.5$ is not exactly constant, whereas the analytical solution in the channel region has been assumed to approach a constant as x approaches x_1. Possibly this assumption is incorrect and an "inner" solution for $x - x_1 = \mathcal{O}\{\epsilon^{1/2}\}$ is

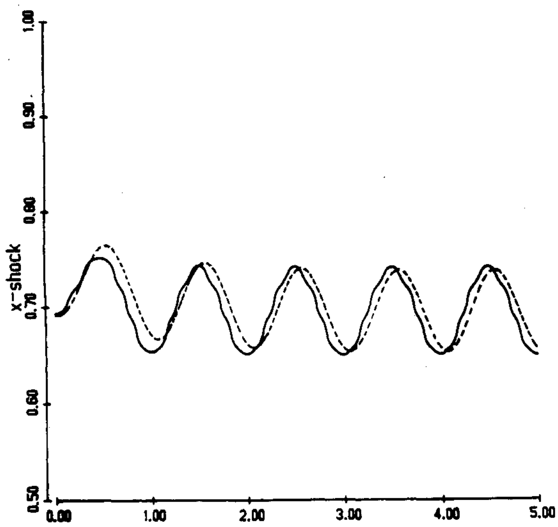

Fig. 2 Shock-wave position as a function of time for unstaggered cascade having parabolic blades of 2% thickness oscillating in pitch with reduced frequency 0.1, amplitude 0.1 deg, and 180-deg phase difference: ——asymptotic solution; -----numerical solution.

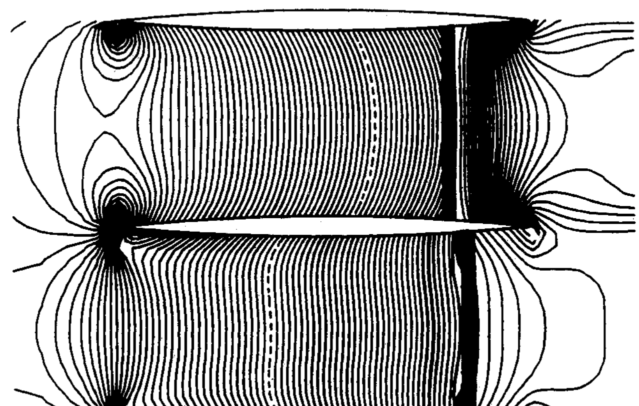

Fig. 3 Numerical solution showing lines of constant Mach number for unstaggered cascade having parabolic blades of 5% thickness oscillating in pitch with reduced frequency 0.5, amplitude 2.5 deg, and 180-deg phase difference; dashed line is $M = 1$.

required for adjustment to a constant back pressure slightly further downstream.

To show further flow details in a particular case, lines of constant Mach number are plotted in Fig. 3 for blades having thickness ratio 5% undergoing oscillations with frequency $\tau^{-1}=0.5$ and amplitude 2.5 deg, at a value of time when the flows in adjacent "channels" are noticeably different. The flows are seen to be nearly one-dimensional except near the entrance and exit and just behind the shock wave. The displacement of the (dashed) sonic line and the shock-wave displacement should probably both be considered $\mathcal{O}(1)$; the amplitudes, however, cannot be determined from a single plot because of the difference in the phase lags. Although $\tau^{-1}=0.5$ should be regarded as $\mathcal{O}(1)$, as already noted, it may be worth recalling that the amplitudes of the sonic-line and shock-wave motions would be predicted by the asymptotic theory of Ref. 1 to be $\mathcal{O}(1)$ if $\tau^{-1}=\mathcal{O}\{\epsilon\}$ and $\alpha=\mathcal{O}\{\epsilon^2\}$.

Concluding Remarks

The computational scheme appears successful in capturing shock waves, but is not capable of resolving vortex sheets sharply. Preliminary calculations for a staggered cascade suggest that the method will be successful for these geometries as well. The asymptotic solutions of Ref. 1 provide fairly good agreement for the shock-wave position provided that the blade thickness ratio and oscillation amplitude are both small enough. Higher-order terms are needed to improve the accuracy for a wider parameter range, and the correct inner solution at the exit is not yet understood. A broader range of numerical calculations is needed to establish whether or not the shock-wave motion has a large effect on the moment for realistic values of the parameters.

References

[1]Messiter, A. F. and Adamson, T. C., Jr., "Forced Oscillations of Transonic Channel and Inlet Flows with Shock Waves," *AIAA Journal,* Vol. 22, Nov. 1984, pp. 1590–1599.

[2]Messiter, A. F. and Adamson, T. C., Jr., "Transonic Small-Disturbance Theory for Lightly Loaded Cascades," *AIAA Journal,* Vol. 19, Aug. 1981, pp. 1047–1054.

[3]Verdon, J. M., "Linearized Unsteady Aerodynamic Theory," *AGARD Manual on Aeroelasticity in Axial Flow Turbomachines,* Vol. 1: Unsteady Turbomachinery Aerodynamics, edited by M. F. Platzer and F. O. Carta, AGARD-AG-298, 1987, Chap. 2.

[4]Acton, E. and Newton, S. G., "Numerical Methods for Unsteady Transonic Flow," *AGARD Manual on Aeroelasticity in Axial Flow Turbomachines,* Vol. 1: Unsteady Turbomachinery Aerodynamics, edited by M. F. Platzer and F. O. Carta, AGARD-AG-298, 1987, Chap. 6.

[5]Li, C.-C., "Unsteady Transonic Cascade Flows," Ph.D. Thesis, The Univ. of Michigan, Ann Arbor, MI, 1988.

[6]Adamson, T. C., Jr. and Messiter, A. F., "Asymptotic Methods for Internal Transonic Flows," NASA Transonic Symposium, 1988.

[7]Kaza, K. R. V. and Kielb, R. E., "Flutter of Turbofan Rotors with Mistuned Blades," *AIAA Journal,* Vol. 22, Nov. 1984, pp. 1618–1625.

[8]Van Leer, B., "Toward the Ultimate Conservation Difference Scheme. V. A Second-Order Sequel to Godunov's Method," *Journal of Computational Physics,* Vol. 32, 1979, pp. 101–136.

[9]Van Albada, G. D., Van Leer, B., and Roberts, W. W., Jr., "A Comparative Study of Computational Methods in Cosmic Gas Dynamics," *Astronomy and Astrophysics,* Vol. 108, 1982, pp. 76–84.

[10]Van Leer, B., "Flux-Vector Splitting for the Euler Equations," *Lecture Notes in Physics,* Vol. 170, 1982, pp. 507–512.

[11]Anderson, W. K., Thomas, J. L., and Rumsey, C. L., "Extension and Applications of Flux-Vector Splitting to Unsteady Calculations on Dynamic Meshes," AIAA Paper 87-1152-CP, 1987.

[12]Hedstrom, G. W., "Nonreflecting Boundary Conditions for Nonlinear Hyperbolic Systems," *Journal of Computational Physics,* Vol. 30, 1979, pp. 222–237.

[13]Giles, M. B., "Nonreflecting Boundary Conditions for Euler Equation Calculations," AIAA Paper 89-1942-CP, 1989.

Suppression of Vortex Asymmetry Behind Circular Cones

Wolfgang Stahl*

Deutsche Forschungsanstalt für Luft- und Raumfahrt, 3400 Goettingen, Federal Republic of Germany

Introduction and Objective

It is a well-documented fact that the flow about a slender body of revolution at zero yaw becomes asymmetric at some high angle of incidence, see e.g., Refs. [1-4]. The initially symmetrical vortex pair on the lee side rearranges into an asymmetric configuration with the asymmetry starting either at the tail of a long afterbody or near the tip of a slender pointed nose. This asymmetric flow leads to a side force acting on the body.

The similar phenomenon of an initially symmetrical vortex pair changing to an asymmetric configuration has been observed long ago on a circular, two-dimensional cylinder, set into motion impulsively in a fluid initially at rest. Behind the cylinder, a symmetrical vortex pair develops in the course of time, growing in size and moving outwards and back until an equilibrium position is reached. After some time, the vortex pair starts to move downstream again and suddenly becomes asymmetric, see e.g., L. Prandtl and O. Tietjens.[5] This type of flow, with the vortices in symmetrical arrangement, was studied theoretically by L. Foeppl[6] using an inviscid flow model. He calculated the equilibrium positions and investigated the stability of the symmetrical vortex pair with respect to small symmetric and antisymmetric displacements from the equilibrium positions (which, in the experiment, were shortly followed by asymmetry of the vortex pair). He found that the symmetrical vortex configuration is stable for symmetric and unstable for antisymmetric disturbances. Results of further theoretical studies of the development of asymmetric flows behind a two-dimensional cylinder and a cone are reported in Refs. 7 and 8, respectively.

It was thought that there was the possibility that inserting a fin between the lee-side vortices may reduce or suppress asymmetry of the vortex flow. Therefore, the flow past a slender circular cone, without and with fin, was studied qualitatively by means of flow-visualization techniques.

Experimental Program

The flow-visualization studies were partly carried out in a water tunnel at Deutsche Forschungsanstalt für Luft- und Raumfahrt (DLR), Goettingen, Federal Republic of Germany, and partly in a wind tunnel at King Fahd University of Petroleum and Minerals (KFUPM), Dhahran, Saudi Arabia. The water tunnel of DLR has a horizontal test section with a cross-sectional area of 0.25 m × 0.33 m. Maximum velocity in the empty test section is $V_\infty \cong 0.5$ m/s. The wind tunnel at KFUPM has a closed horizontal test section with a cross-sectional area of 0.8 m × 1.1 m. Maximum velocity in the empty test section is $V_\infty = 35$ m/s. The basic circular cones had

Received June 22, 1989; presented in extended form as Paper 89-3372 at the AIAA Atmospheric Flight Mechanics Conference, Boston, MA, Aug. 14–16, 1989; revision received Sept. 28, 1989.

Copyright © 1989 by the American Institute of Aeronautics and Astronautics, Inc. All rights reserved.

*Scientist, Institute of Experimental Fluid Mechanics; currently Professor, Department of Mechanical Engineering, King Fahd University of Petroleum and Minerals, Dhahran 31261, Saudi Arabia. Affiliate Member AIAA.